Evaluation of Taguchi's Approach for Malachite Green Removal Using Electrocoagulation with Varying Electrode Connections

Samlan Hussein Abbas[1*], Haydar Fadhel[1], Farooq Al-Sheikh[1], Iftikhar Ali Hussein[2]Alhassan H Ismail[3]

[1]College of Chemical Engineering, University of Technology, Baghdad, Iraq
[2] Engineering Technical College, Middle Technical University, Baghdad, Iraq
[3] Middle Technical University, Polytechnic College of Engineering, Baghdad, Iraq

*Corresponding Author: Email: salman.h.ali@uotechnology.edu.iq

Abstract

This study investigated the removal of Malachite Green (MG) from water through electrocoagulation (EC) using Fe–Fe, Al–Al, and Al–Fe electrode setups. The Taguchi method, employing an L25 (5^5) orthogonal array, focused on optimizing five key factors: current density (0.2–1.0 mA/cm²), pH (3–10), initial dye concentration (10–100 mg/L), distance between electrodes (5–25 mm), and duration (5–60 min). Signal-to-noise (S/N) ratio and ANOVA evaluations indicated that pH (10) with Fe-Fe electrodes and current density (0.8 mA/cm²) with Al-Al electrodes were the most significant variables. Increasing the initial dye concentration or the distance between electrodes raised the voltage and consistently increased the removal percentage (%R). Enhancing electrolyte concentration initially improved color removal %R to a certain extent, after which no further enhancements were observed. In terms of efficient MG removal from water, the Fe-Fe, Al-Al, and Fe-Al configurations demonstrated efficiencies ranging from 12.59% to 98.6%. The initial concentration had a substantial impact on results (with ANOVA contributions of 44.3% to 34.9%), closely followed by the duration of electrolysis. Optimal conditions yielded 88% to 100% removal with less than 3% deviation from predicted values. The maximum conditions for color removal varied based on electrode material: pH (10, 8, and 10), current density (1.0, 0.8, and 0.8 mA/cm²), contact time (20, 60,and 60 min), distance between electrodes (20, 15,and 15 mm), and initial concentration (100 mg/L). The ideal salt concentration was determined to be 0.1 g/L, with an optimal stirring speed of 150 rpm. The Taguchi design effectively optimized EC performance, recommending Fe-Fe electrodes for superior efficiency compared to Al-Al and Fe-Al setups.

Keywords: Electrocoagulation, Malachite Green, Electrode type, Taguchi method, Optimization, ANOVA, Wastewater treatment

1. Introduction

The rapid growth of industries like textiles, paper, leather, plastics, and food leads to significant colored effluent discharge, posing a major environmental issue [1]. These effluents contain complex, non-biodegradable synthetic organic dyes that are aesthetically harmful, especially at low concentrations, and are highly visible pollutants [2, 3]. Their presence impedes sunlight penetration, disrupts aquatic photosynthesis, and can contribute to oxygen imbalance [4, 5]. Additionally, many dye compounds are toxic, persistent, and carcinogenic [6-8]. Synthetic dyes enter water bodies due to untreated industrial effluents, a common practice. Their presence, even in low concentrations, is undesirable [9, 10]. Many synthetic dyes exhibit teratogenicity, mutagenic, and carcinogenic properties [11, 12].

Malachite Green (MG) is a widely recognized cationic triphenylmethane dye that finds extensive applications in both textiles and aquaculture, particularly for diverse materials such as fleece, silk, cotton, and leather products. It is well-regarded for its stability and vibrant coloration, which contribute to its popularity in industrial processes [13]. However, this dye also raises significant health concerns due to its potential adverse effects on the immune system, implications for reproduction, possibilities of geno toxicity, and associated risks of carcinogenicity. These serious health issues have led to ongoing disputes and controversies surrounding its continued use in various sectors [14].

Conventional methods for treating dye-polluted water include ozonation, adsorption, membrane filtration, ion exchange, advanced oxidation processes, chemical coagulation (generating large secondary sludge), and biological treatment (often hindered by dye toxicity). These methods can be ineffective, costly, unsustainable, and produce excessive solid waste requiring further treatment [15]. Electrocoagulation (EC) is an emerging physico-chemical treatment method noted for its ability to produce coagulants on-site with sacrificial metal electrodes [16]. EC boasts advantages such as easy operation, minimal sludge output, high removal efficiency, and no need for chemical additives [17].

The impact of malachite green on various biological aspects, including immunity, reproduction, and the potential for genotoxicity, has resulted in significant debate regarding its use in different applications and settings. This controversy surrounding its safety and effectiveness continues to be a topic of discussion [18]. Coagulation is the main technique employed in the treatment of drinking water, which serves the vital purpose of eliminating harmful contaminants from the water [19].

Wastewater with dyes can be treated by techniques like ozonation, incineration, advanced oxidation, adsorption, and biological treatment. However, these methods are often ineffective, costly, environmentally harmful, and generate excessive sludge that requires further treatment [20]. The intricate and complex process of Environmental Chemistry (EC) meticulously removes various harmful pollutants from wastewater through numerous sophisticated mechanisms that work together in harmony [21].

The process involves electrolysis of metallic anodes, leading to easily separable metallic hydroxides and pollutant coagulates. Electro-coagulation outperforms conventional methods

by effectively removing tiny colloidal particles [22]. Iron and aluminum are popular due to their availability and low cost. They dissolve at the anode, forming -OH ions and H_2 at the cathode, generating an in-situ coagulant, as shown in the equations [23].

$$M \rightarrow M^{+1} + e^{-1} \quad (1)$$

$$2H_2O\ (l) + 2\ e^{-1} \rightarrow 2OH^{-1} + H_2\ (g) \quad (2)$$

$$M^{+1} + OH^{-1} \rightarrow Mn\ (OH)\ (s) \quad (3)$$

Electrochemical separation (EC) involves four main steps: (1) oxidation at the anode produces metal cations; (2) electrolysis at the cathode generates hydroxide and hydrogen bubbles; (3) metal ions react with OH to form compounds; and (4) hydroxyl metal adsorbs pollutants, forming coagulants separated by Coagulation/Flocculation [24]. The performance and efficiency of EC depend on factors like initial concentration, pH, current density, treatment time, and electrode arrangement. Optimizing these parameters is crucial for maximizing pollutant removal and minimizing costs [25].

Conventional optimization methods tend to be quite resource-heavy and often fail to adequately capture the intricate and complex interactions that may exist among independent variables [26]. The Taguchi Design of Experiments (DOE) method was specifically chosen for this study to effectively analyze and interpret the influence of multiple control factors at different levels by utilizing an orthogonal array for systematic investigation [27].

The comprehensive analysis employs the Signal-to-Noise (S/N) ratio effectively to determine the optimal conditions that enhance removal efficiency significantly while also ensuring the stability and robustness of the overall process [28]. Taguchi's Design of Experiments (DOE) offers an efficient method for optimizing multivariable systems with fewer experiments. Utilizing orthogonal arrays and signal-to-noise (S/N) analysis, it highlights key factors impacting system response and finds optimal conditions. This contrasts with traditional one-factor studies, as Taguchi DOE minimizes experimentation time, cost, and errors [29, 30].

This work aims to optimize the EC process for MG removal using three electrode connections Iron-Iron (Fe-Fe), Aluminum-Aluminum (Al-Al), and mixed Fe-Al systems through the Taguchi framework. Taguchi orthogonal array evaluates pH, initial concentration, internal distance electrodes, current density, and electrolysis time in three configurations. S/N analysis and ANOVA identify optimal conditions and quantify parameter contributions, enhancing understanding of electrode connection effects on dye removal. This research addresses a gap regarding the simultaneous effects of factors on electrode systems, with key objectives of evaluating and identifying optimal operational parameters for each type.

2. Materials and Methods

2.1. Materials

Malachite green dyestuff was obtained from Sigma Aldrich, with properties listed in Table 1. Aluminum or Iron electrodes sized 46.9 × 95 × 0.1 mm and with a 175.08 cm^2 active surface area were used. Instruments included a digital power supply Tp-1305EC, an Al Kawther power supply, a magnetic stirrer, a pH meter, a centrifuge, and a visible spectrophotometer.

Table 1. Properties of Malachite Green dye.

Molecule Formula	$C_{52}H_{54}N_4O_{12}$
Molecular Weight, g/mol	927.03
Wavelength (λ)	616-620 nm
Dye types	Cationic dye, Azo dye (N=N)
IUPAC name	Triphenylmethane category

2.2 Methods

The electrocoagulation method evaluated color removal from a lab-prepared aqueous dyestuff solution. A 1000 mg/l stock solution was diluted with distilled water and stored in cold, dark conditions. To prepare the MG stock solution, a specific quantity of dye was dissolved in distilled water and measured using a volumetric flask. This 1000 ml of distilled water was then gradually diluted to achieve the desired concentrations of Malachite Green, ranging from 10-100 ppm. Various factors including dyestuff concentration, electrolyte amount, current density, pH, mixing speed, electrode distance, and electrolysis time were analyzed to determine optimal conditions. In the reactor, two electrodes (one anode and one cathode) were used in a monopolar configuration. The electrode distance was set at 15 mm for Fe-Al and Al-Al, and 20 mm for Fe-Fe. Chemicals 1 M HCl and 1 M NaOH were used to adjust the pH, and the electrodes were cleaned in a solution beforehand. They were cleaned with distilled water, dried, and prepared for weighing. Five-milliliter samples were centrifuged for five minutes at 4000 rpm and measured at 620 nm. The calculations from this study used orthogonal arrays for experimental design with the Taguchi method, detailed in Table 2.

$$J = \frac{I}{2S} \quad (4)$$

The current density (J, mA/cm^2), current intensity (I, mA), and electrode area (S, cm^2) were analyzed for their effects on MG adsorption from aqueous solutions. The Taguchi method helped identify key variables and optimal concentrations, as shown in Table 2.

Table 2: Chosen experimental parameters and levels.

Factor	Symbol	Levels values
I.C., mg/l	X1	10, 20, 40, 80, and 100
Acidity, pH	X2	3, 5, 7, 8, and 10
Time, min	X3	5, 10, 20, 40, and 60
C.D, mA/cm^2	X4	0.2, 0.4, 0.6, 0.8, and 1.0
D. E., mm	X5	5, 10, 15, 20, and 25

When using the Taguchi method, the experiment design is as follows:

1. The quality attributes that needed to be optimized were found to be the % removal and the adsorption capacity. By gradually diluting the stock solution with distilled water, experimental solutions with the required concentrations were obtained. [31]

2. Deciding on the alternative levels of the controllable factors that can be maintained and set. The design factors in this paper are pH, and contact time, adsorbent dose, starting MG concentration, and five levels of each factor. [32]

3. The experiment was conducted using values of the design information combined by MINITAB, V. 21, by using the Taguchi method as the design of the experiment (DOE), as demonstrated in selecting the orthogonal array and creating it. The L_{25} (5^5) orthogonal array experiment was chosen as displayed in Table 3.

Table 3: L_{25} orthogonal designs, Levels of five factors,

Run	**I.C, ppm** x_1	**pH** x_2	**Time, min** x_3	**C.D, mA/cm^2** x_4	**D.E, mm** x_5
1	10	3	5	0.2	5
2	10	5	10	0.4	10
3	10	7	20	0.6	15
4	10	8	40	0.8	20
5	10	10	60	1.0	25
6	20	3	10	0.6	20
7	20	5	20	0.8	25
8	20	7	40	1.0	5
9	20	8	60	0.2	10
10	20	10	5	0.4	15
11	40	3	20	1.0	10
12	40	5	40	0.2	15
13	40	7	60	0.4	20
14	40	8	5	0.6	25
15	40	10	10	0.8	5
16	80	3	40	0.4	25
17	80	5	60	0.6	5
18	80	7	5	0.8	10
19	80	8	10	1.0	15
20	80	10	20	0.2	20
21	100	3	60	0.8	15
22	100	5	5	1.0	20
23	100	7	10	0.2	25
24	100	8	20	0.4	5
25	100	10	40	0.6	10

4. As part of the planned orthogonal experiment, a sequence of experiments was carried out one after the other.

$$\text{Removal}\% = \frac{C_i - C_t}{C_i} \times 100 \quad (5)$$

Where Removal% is the dye removal percentage, and C_i and C_t are the dye concentration at initial and at time, t.

5. Experiments were conducted and response values were acquired in the second stage. By earlier research, response values were transformed into the S/N ratio for result analysis, as Equation 6, the larger the better quality characteristic was applied in this study [33].

$$S/_N = -10 \log\left(\frac{1}{n}\sum_{i=1}^{n}\frac{1}{y^2}\right) \quad (6)$$

Where y measures percentage removal, n indicates repetitions, and S/N is the signal-to-noise ratio. The subscript SB signifies large-the-better. Ideal conditions were established by determining the average I(S/N) SB ratio for each controllable factor at level (i), known as (S/N) FL. The S/N ratio is a key performance metric in Taguchi design, employing the phrases "The larger is better," "The smaller is better," and "The nominal is better," with the optimized process aiming for the maximum output of "the larger is better." S/N ratios were computed with Equation 6. Malachite Green removal efficiencies determined performance parameters in the Taguchi design, emphasizing "The larger is better."

3. Results and Discussion

3.1 Experimental removal performance

Malachite Green (MG) removal was assessed using Taguchi L25 (5^5) design with five variables: initial concentration (X1), pH (X2), electrolysis time (X3), current density (X4), and inter-electrode distance (X5). Experiments utilized three electrode configurations: Fe–Fe, Al–Al, and Al–Fe, achieving removal efficiency between 12.59% and 98.6%, highlighting the effectiveness of electrocoagulation.

3.2 Optimization Parameters (Signal-to-Noise (S/N) ratios)

In the investigation's early phases, the Taguchi method is recommended to screen input variables using signal-to-noise (S/N) ratios ("Larger-the-Better") for factor influence evaluation. Analysis of Tables (4, 5, and 6) show that pH and time are the most significant factors. Maximum electrocoagulation efficiency occurs at pH 8 and 10, with optimum times varying between 20 and 60 minutes for different materials. Deviations reduce efficiency [34].

Table 4: Response table for Signal-to-Noise Ratios for (Fe-Fe)

Larger is better					
Level	C.I.	pH	Time	C.D.	D. E.
1	33.44	30.98	32.80	32.68	34.87
2	35.85	35.12	33.33	35.18	34.80
3	36.35	35.65	35.23	36.29	36.73
4	34.77	36.48	36.67	36.56	35.74

5	36.32	38.51	38.70	36.02	34.59
Delta	2.91	7.53	5.90	3.88	2.14
Rank	4	1	2	3	5

Table 5: Response table for Signal-to-Noise Ratios for (Al-Al)

Larger is better					
Level	C.I.	pH	Time	C.D.	D. E.
1	32.44	32.19	32.63	33.37	33.45
2	38.46	38.17	37.59	37.78	37.97
3	38.48	38.66	38.60	37.99	38.82
4	38.68	38.67	38.81	39.18	38.27
5	38.79	39.17	39.22	38.54	38.35
Delta	6.35	6.98	6.59	5.81	5.37
Rank	3	1	2	4	5

Table 6: Response table for Signal to Noise Ratios for (Al-Fe)

Larger is better					
Level	C.I.	pH	Time	C.D.	D. E.
1	33.51	30.85	32.54	33.64	33.81
2	35.27	36.25	34.35	36.25	35.93
3	36.45	37.38	36.45	35.92	37.19
4	37.03	37.78	37.64	37.42	35.85
5	37.43	37.43	38.71	36.47	36.92
Delta	3.92	6.93	6.18	3.78	3.38
Rank	3	1	2	4	5

This observation was supported by literature, using the highest S/N ratio across control levels to determine optimal levels for factors. For (Fe-Fe) electrodes, optimal levels were I.C. (Level 5, S/N ratio = 36.32 and Level 3, S/N ratio = 36.35), pH (Level 5, S/N ratio = 38.77), C.D. (Level 5, S/N ratio = 38.63), and D.E. (Level 4, S/N ratio = 36.73) with time at Level 3 (S/N ratio = 36.27), as shown in Table 6. For (Al-Al) electrodes, the optimal levels were I.C. (Level 5, S/N ratio = 38.79), pH (Level 5, S/N ratio = 39.17), C.D. (Level 4, S/N ratio = 39.18), and D.E. (Level 3, S/N ratio = 38.82) with time at Level 5 (S/N ratio = 39.22), indicated in Table 7. For (Al-Fe) electrodes, the optimum levels were I.C. (Level 5, S/N ratio = 37.43), pH (Level 4, S/N ratio = 37.78), C.D. (Level 4, S/N ratio = 37.42), and D.E. (Level 4, S/N ratio = 37.42) with time at Level 5 (S/N ratio = 38.71), as per Table 7. The best removal efficiency was found at pH = (8,10), j = (0.8, 1.0) (mA cm–2), t = 20.6 min, with I.C. 100 mg/l and D.E. at 15.20 mm. The Taguchi method applied different steps for analysis, transforming response values into the S/N ratio, which was used to evaluate Figures 1, 2, and 3. In electrocoagulation, the goal is "Larger is better," as maximum recovery and color removal percentages are desired. The S/N value for each response was calculated using the S/N ratio formula in step (5). [35]

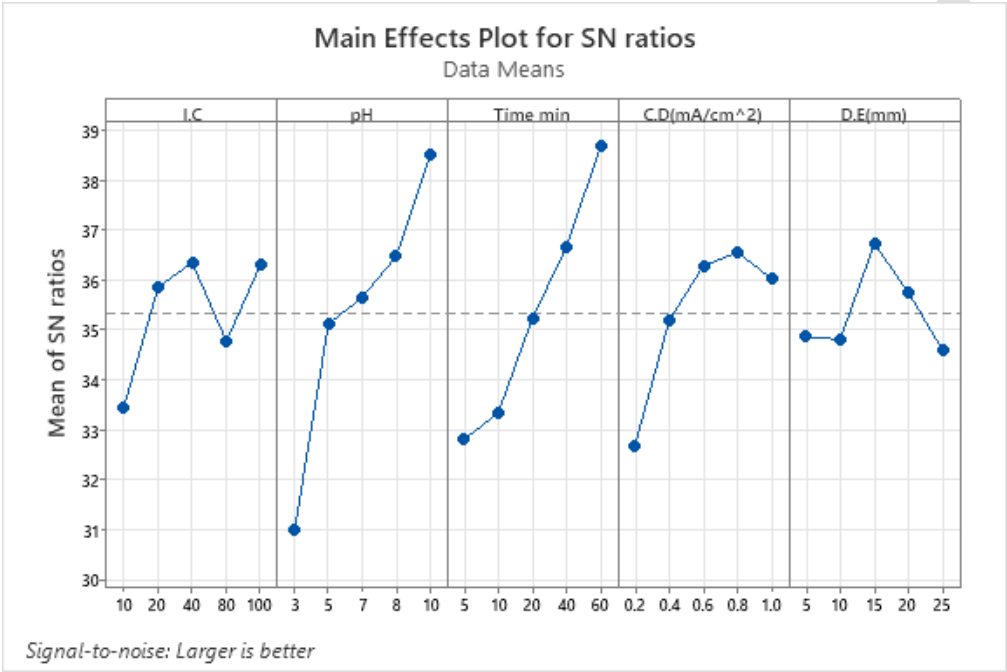

Figure 1: Taguchi Analysis: %R versus I. C., pH, C.D., D.E., Time for (Fe-Fe).

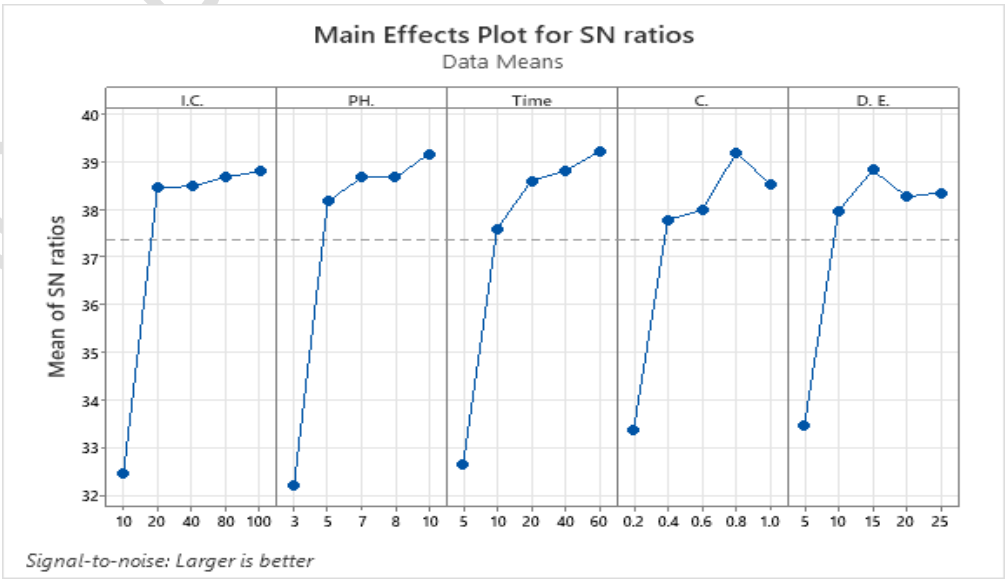

Figure 2: Taguchi Analysis: [%R versus I.C., pH., Time, C., and D. E. for (Al-Al)].

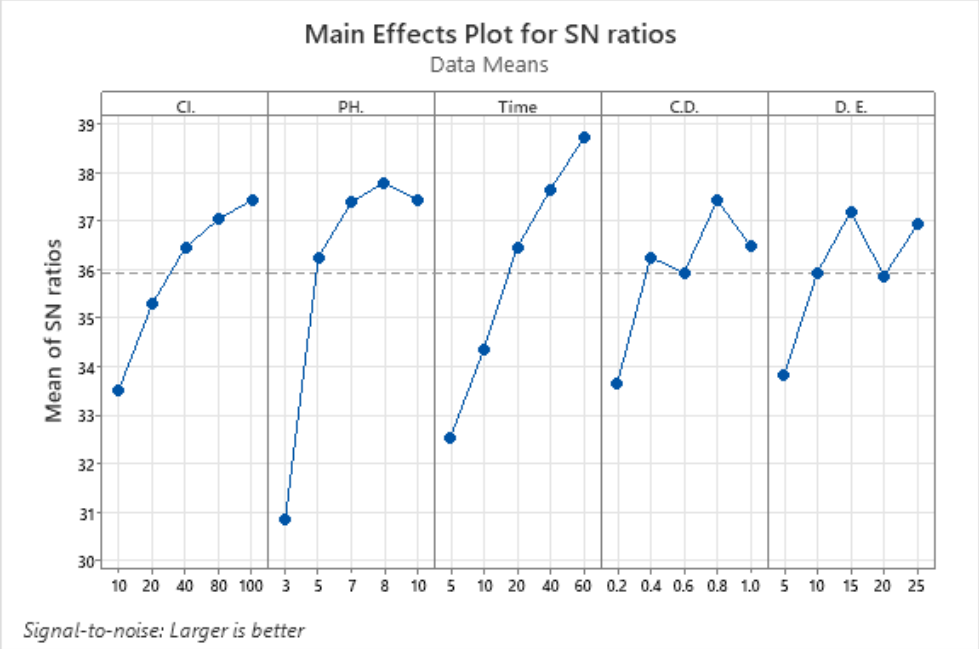

Figure 3: Taguchi Analysis: [%R versus I. C., pH, C.D., D.E., Time for (Al-Fe)].

3.3 Effect of Operating Parameters on MG Removal

Taguchi analysis showed that electrolysis time and pH significantly affect MG removal ($p < 0.05$). Extended electrolysis time boosts coagulant production, destabilizing dye molecules for better removal. Optimal pH ranges from acidic to neutral, where stable metal hydroxide flocs effectively capture dyes. Higher current density enhances removal by increasing ion dissolution; however, excessive levels lead to electrode passivation and energy loss [36]. Initial dye concentration affected removal efficiency, with lower concentrations yielding better results. Higher dye levels necessitated longer treatment times. Increased NaCl enhanced conductivity and bubble generation, boosting coagulation efficiency [37].

3.4 Comparison between Electrode Types

Fe–Fe electrodes showed the highest removal efficiency (>99%), then Al–Al (>97%) and Al–Fe (>90%). Iron electrodes created denser, stronger flocs with improved settling. Al formed smaller, highly charged flocs effectively removing MG. Mixed Al–Fe maintained moderate performance due to varying dissolution rates. ANOVA indicated that pH and electrolysis time were statistically significant across all systems ($p < 0.05$). [38].

Table 7 presents the experimental results and S/N ratio for each run. To assess each factor's effect on color removal, the S/N ratio was averaged across various intensities. The mean S/N ratio for each factor was computed and plotted, with peak points indicating ideal conditions. Figures (1, 2, and 3) illustrate the Taguchi analysis: %R versus I. C., pH, C.D., D.E., and Time for (Fe-Fe), (Al-Al), and (Al-Fe), showing optimal conditions for the EC process's color removal. As a result;

Fe–Fe: Initial concentration (X1) = 44.3%, Time (X3) = 17.1%, pH (X2) = 13.3%, Current density (X4) = 12.3%, Distance (X5) = 9.5%
Al–Al: X1 = 40.5%, X3 = 26.3%, X4 = 13.1%, X2 = 11.5%, X5 = 8.6%
Al–Fe: X1 = 34.9%, X3 = 28.0%, X2 = 17.3%, X4 = 11.8%, X5 = 6.4%
Sensitivity analysis results indicate that initial concentration is the most influential parameter, with electrolysis time next. Electrode spacing had the least impact across all configurations. [39].

Table 7: Experimental results obtained.

Expt.%R (Fe-Fe)	S/N_{SB} ratio (Fe-Fe)	Predict %R (Fe-Fe)	Expt.%R (Al-Al)	S/N_{SB} ratio (Al-Al)	Predict %R (Al-Al)	Expt.%R (Al-Fe)	S/N_{SB} ratio (Al-Fe)	Predict %R (Al-Fe)
12.59	13.25	15.01	3.50	10.88	9.96	8.20	18.27	14.24
36.5	32.21	33.33	57.50	35.19	54.48	47.03	33.44	43.76
66.29	33.51	65.43	82.80	38.36	77.59	73.57	37.33	73.43
75.6	38.88	76.55	87.90	38.87	86.12	90.86	39.16	88.55
98.29	39.49	99.97	88.00	38.88	88.50	92.50	39.32	92.19
34.99	29.57	35.25	60.70	35.66	61.60	26.70	28.53	26.40
53.59	33.16	56.01	94.90	39.54	100	64.90	36.24	70.94
83.59	39.41	80.43	91.00	39.18	91.56	77.10	37.74	73.83
75.89	36.23	75.03	94.80	39.53	89.62	81.50	38.22	81.35
77.19	39.45	78.15	83.00	38.38	81.22	60.43	35.62	58.12
40.09	34.64	41.05	73.20	37.29	71.39	45.26	33.11	42.96
64.89	35.57	65.57	87.40	38.83	88.30	74.50	37.44	74.19
87.79	38.04	90.21	91.3	39.20	97.77	84.88	38.57	90.92
62.19	35.35	59.03	73.80	37.36	73.36	68.97	36.77	65.69
86.19	37.51	85.33	96.80	39.71	91.62	65.55	36.33	65.41
36.69	28.13	35.83	76.40	37.66	71.22	60.13	35.58	59.98
83.39	39.76	84.35	89.40	39.02	87.62	85.92	38.68	83.62
46.09	32.31	46.77	82.20	38.29	83.10	67.47	36.58	67.17
53.49	33.17	55.91	90.00	39.08	96.43	68.85	36.75	74.89
65.39	37.52	62.23	92.60	39.33	92.16	75.60	37.57	72.31
85.69	39.60	82.53	93.90	39.45	93.46	86.78	38.76	83.50
56.79	33.17	55.93	81.70	38.24	76.52	59.05	35.42	58.91
36.49	34.04	37.45	82.00	38.27	80.22	68.13	36.66	65.83
68.89	36.13	69.57	83.80	38.46	84.70	79.45	38.00	79.14
98.6	39.87	100.0	94.60	39.51	100	82.04	38.28	88.09

3.5 Effect of Operating Parameters on the MG Removal

The removal efficiency of MG was significantly influenced by all operating parameters (X1–X5), as confirmed by S/N ratios and ANOVA ($P < 0.05$).

The Taguchi results indicated that the operating parameters significantly affect Malachite Green (MG) removal efficiency in the electrocoagulation (EC) process. pH was the most influential parameter, followed by current density and electrolysis time, with salt concentration being the least significant. The significance rankings and p-values ($P < 0.05$) confirm that not all parameters impact the removal mechanism equally [40].

3.5.1 Initial dye concentration(X1)

Solutions with concentrations of 10-100 mg/l were prepared for electrocoagulation using Fe-Fe, Al-Al, and Al-Fe electrodes to evaluate removal efficiencies for dyestuff. Process parameters included an original pH of 3-10, NaCl concentration at 100 mg/L, stirring speed of 150 rpm, current density from 0.2-1.0 mA/cm2, electrode distance of 5-25 mm, and electrolysis time of 5-60 minutes. Removal efficiency increased with concentration; however, higher MG concentration reduced %R for all electrodes: Fe–Fe (12.59 → 98.6%), Al–Al (35.2 → 100%), and Al–Fe (26.4 → 92.5%).

Initial dye concentration significantly impacted all electrode systems. Raising MG concentration from 10 to 100 mg/L led to a drop in % removal. For Fe–Fe electrodes, removal fell from 98.6% to 12.59%, as higher dye loads saturated coagulant sites, impairing floc efficiency. Al–Al electrodes displayed a similar pattern, with slightly higher maximum removal due to Al $(OH)_3$ flocs' adsorption capacity. The hybrid Al–Fe system showed moderate reductions, indicating that combined Fe and Al hydroxides offer complementary removal pathways.

At high concentration, the dye molecules increase significantly compared to low concentration, resulting in higher % R[41]. The S/N ratios for (Fe-Fe) electrodes increase from (33.44-36.32, 36.35), (Al-Al) from (32.5-38.8), and (Fe-Al) from (33.5-37.5).

As a result, for Statistical significance**:** when $P < 0.05$ for all three systems, confirming X1 as the most critical parameter. ANOVA contributions were highest for X1: Fe–Fe (44.3%), Al–Al (40.5%), Al–Fe (34.9%)., $P < 0.05$ for all electrodes; X1 is the dominant factor [42].

3.5.2. Mixing speed

Stirring accelerates ion movement in the electrocoagulation cell and prevents concentration gradients, enhancing pollutant removal efficiency. The optimal mixing speed was determined using a magnetic stirrer at 100, 150, 200, 250, and 300 rpm. The removal efficiency increased with mixing speeds up to 150 rpm, where more energy was required for mixing. However, efficiency decreased past this speed to 300 rpm. Figure 4 illustrates how mixing speed affects energy use and color removal, confirming 150 rpm as the optimal speed [43].

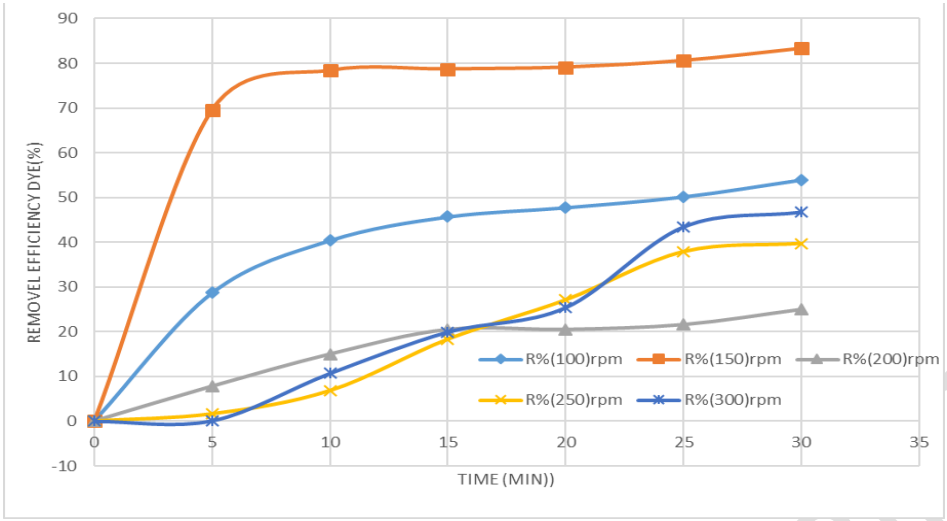

Figure 4: Optimum stirring speed used in experiments for Al-Al, [I.C. (50mg/l), pH (8), Time (30min), Current (0.20 A), and Distance (0.5cm)].

3.5.3. Current density(X4)

Current density was the second most influential factor. Higher currents enhance electrode material dissolution and bubble generation, boosting dye aggregation and flotation. However, excessive current leads to unnecessary energy use and less effective removal due to smaller flocs from aluminum ion overdosing. Statistical analysis confirmed current density's significance ($P < 0.05$) [44].

The electrocoagulation efficiency, coagulation rate, and bubble generation rate are affected by current density. Increased current density raises the anodic dissolution rate, significantly impacting removal efficiency. The optimal current density was determined after establishing the mixing speed, using settings of (0.2, 0.4, 0.6, 0.8, and 1.0) mA/cm².Higher current density improves removal efficiency, but energy requirements also increase [45]. The difference between current density and efficiency does not significantly rise near the maximum value. The optimal current density was identified as 0.8 mA/cm², as removal values for Fe-Fe and Al-Fe are similar. Higher densities boost coagulant generation and hydrogen bubble formation, enhancing MG destabilization and flotation. Optimal densities were 0.8–1.0 mA/cm² for Fe-Fe and Al-Fe, while Al-Al showed lower sensitivity, likely due to slower Al dissolution kinetics [46].

As a result, in the context of Statistical significance, we find that for the Fe–Fe system, the P-value is 0.06, which is greater than 0.05, indicating it is less significant in terms of its statistical impact. On the other hand, for the Al–Al system, the P-value is recorded at 0.04, which is notably less than 0.05 and thus indicates that it is considered statistically significant. Furthermore, for the Al–Fe pairing, the P-value stands at 0.05, which is approximately equal to 0.05, categorizing it as borderline significant. This analysis clearly illustrates that the current density has a greater influence in systems that contain aluminum, particularly highlighting the Al–Al electrode configurations as being especially impactful and relevant in this regard [47].

3.5.4. pH(X2)

The pH had the strongest effect on MG removal, being the most influential factor. Acidic conditions boosted aluminum dissolution from the anode, leading to more $Al(OH)_3$ flocs that destabilized the dye. A slight increase toward neutral pH reduced efficiency, while alkaline conditions decreased performance due to soluble Al species affecting coagulation. Thus, pH is a statistically significant variable ($P < 0.05$) and crucial for the electrocoagulation process, impacting reactions and involving both the anode and cathode. The pH value was determined after measuring current density. Solutions of pH 3, 5, 7, 8, and 10 were prepared. It was observed that as pH approached higher values, the difference in removal efficiency diminished. The removal efficiencies were 94.5%, 77.9%, and 40% at pH 3 and 5 after 20 minutes. pH 8 and 10 were identified as ideal, with processing time unaffected by pH variations. The main effects plot for S/N ratios demonstrates that pH shifts significantly influence color removal and usage. Optimal dye removal occurs in mildly acidic to neutral pH levels: Fe–Fe at pH 7 maximizes floc formation and MG removal; Al–Al at pH 5–7 optimizes Al $(OH)_3$ solubility; and Al–Fe at slightly higher pH (7–8) balances hydroxide formation. Extreme pH levels reduce removal due to destabilization.

As a result, when it comes to Statistical significance; for the Fe–Fe comparison, we find $P = 0.03$, which is less than 0.05, indicating a significant result; for the Al–Al pairing, the value is $P = 0.08$, exceeding 0.05, suggesting a moderately significant outcome; finally, for the Al–Fe evaluation, we observe $P = 0.04$, which is less than 0.05, denoting a significant finding. This indicates that pH is particularly important for Fe–Fe and Al–Fe systems, less so for Al–Al electrodes [48].

3.5.5. Distance between electrodes(X5)

The impact of electrode spacing on removal efficiency was examined by varying distances between them (5, 10, 15, 20, and 25 mm). Results showed that increasing the distance reduced removal efficiency and increased energy consumption. The highest yield occurred in the 15 - 20 mm range, as shown by the removal graph. Figures 1, 2, and 3 illustrate how electrode distance impacts energy consumption and color removal. Electrode spacing affects bubble formation, mass transfer, and electric field distribution. In the 5–25 mm range, its impact on % removal was minor: Fe–Fe (9.5%); Al–Al (8.6%); and Al–Fe (6.4%).

As a result, based on our analysis of Statistical significance, we found that for P values greater than 0.05 across all types of electrodes, this indicates a clear finding that within the specific range we selected, X5 does not play a critical or essential role. The observed effect was found to be minor across all electrode types and conditions (with $P > 0.05$), further confirming that spacing is not critical or significant when considering distances ranging from 5 to 25 mm [49].

3.5.6. Electrolysis time(X3)

Electrolysis time moderately influenced removal efficiency, with longer durations ensuring adequate coagulant release and charge neutralization. However, beyond an optimum duration,

no significant increase is noted as dye molecules destabilize. Time is statistically significant ($P < 0.05$), showing that exceeding the optimum yields minimal added benefit. The production of ions and hydroxide flocs varies with electrolysis time. Earlier experiments indicated that twenty minutes is ideal. As time progressed, removal efficiency increased: Fe–Fe %R rose from 12.6% (5 min) to 98.6% (60 min); Al–Al from 35.2% to 100%; Al–Fe from 26.4% to 92.5%. Extended time aids destabilization, yet overly long operations can be inefficient.

Statistical significance was $P < 0.05$ for all systems, confirming time as the second most influential factor (ANOVA contributions: Fe–Fe 17.1%, Al–Al 26.3%, Al–Fe 28.0%). Increased duration enhanced removal efficiency through floc growth, significant across electrodes ($P < 0.05$). Higher current densities boosted coagulant production and flotation, significant in Al–Al ($P=0.04$), borderline in Al–Fe ($P\approx0.05$), and less so in Fe–Fe ($P=0.06$) [50].

3.5.7 Overall Significance and Comparison

pH had the greatest effect on dye removal efficiency, followed by current density and electrolysis time, while salt concentration was the least significant. Controlling pH and current density is crucial. This conclusion supports reaction chemistry principles, confirming that optimal destabilization and coagulation primarily rely on aluminum species formed at suitable pH and current levels. Table 8 clearly ranks the significance of factors across electrode systems based on ANOVA and P-values.

Table 8: Comparative significance across electrode systems based on ANOVA and P-values

Factor	Symbol	Fe-Fe	Al-Al	Al-Fe
Initial conc.	X1	Most significant $P < 0.05$	Most significant $P < 0.05$	Most significant $P < 0.05$
pH	X2	Significant $P < 0.05$	Most significant $P < 0.05$	Most significant $P < 0.05$
Time	X3	Significant $P < 0.05$	Moderately significant	Significant
Current density	X4	Less significant	Significant	Borderline significant
Distance between electrodes	X5	Not significant	Not significant	Not significant

Initial concentration influences all systems most; Time is key for Al-containing electrodes; pH matters for Fe–Fe and Al–Fe, less for Al–Al; Current density is critical for Al electrodes, while Electrode distance has minimal impact.

In conclusion, the Fe–Fe and Al–Al combinations demonstrate notably higher removal efficiency with varying sensitivity patterns in their performance metrics, while the Al–Fe combination provides a more balanced and stable removal across different conditions, ensuring consistent and reliable performance under a range of scenarios [51].

3.6 Calculations Based on Optimum Values

The Taguchi method calculates the Signal-to-Noise ratio (S/N) for quality and uses an orthogonal array for experimental design. This array consists of experimental combinations that share equal probability and controllable factors. Results showed optimization in the experimental combinations, with removal rates of 98.78% for Fe-Fe electrodes, 95.7% for Al-Al, and 96.7% for Al-Fe, as illustrated in Figure 5.

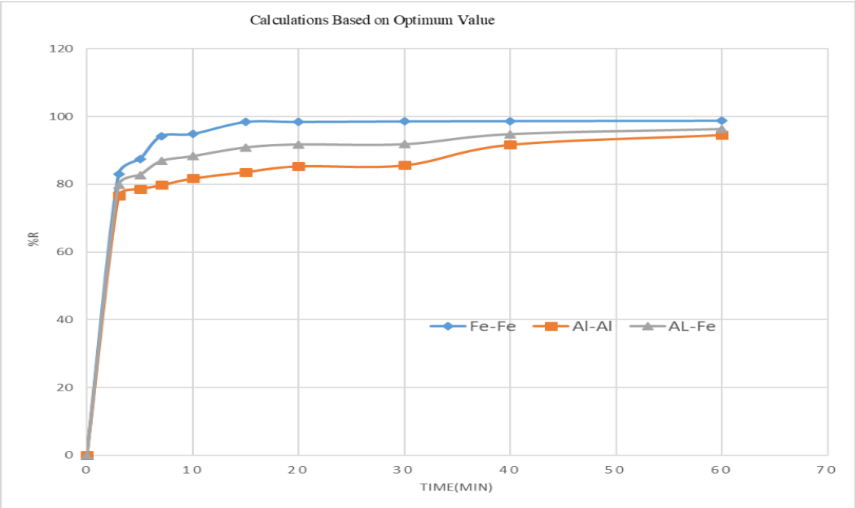

Figure 5: Calculations Based on Optimum Values, [C salt=100 mg/L, 150 rpm, C_0 100mg/L original pH (8), for Al-Fe, pH (10) for (Al-Al) (Fe-Fe); electrodes distance 20mm for (Fe-Fe) and (15mm), for (Al-Al) & (Al-Fe)]

The current density set at 0.8 (mA/cm^2) was observed for both configurations, Al-Al and Al-Fe, while a higher current density set at 1.0 (mA/cm^2) was recorded for the Fe-Fe configuration. These results were concluded after duration of 60 min. The outcomes depended significantly on the carefully structured experimental design implemented using the Taguchi method [52].

3.7 Analysis of Variance (ANOVA)

ANOVA was conducted to assess the significance of factors at 95% confidence ($P < 0.05$) using Minitab 21.0 software. This analysis pinpointed key variables that can enhance removal and adsorption capacity, allowing for optimal values to be selected. ANOVA tested the impact of model components on removal efficiency at a 5% significance level.Model reduction relies on statistical significance. A parameter with a p-value under 0.05 indicates significant effect and stays in the model; otherwise, it is removed.An ANOVA was conducted to determine the significance of process parameters, with findings in Tables 4, 5, and 6. S/N ratio analysis follows a similar pattern. The significance ranking indicates that for %R efficiencies, initial pH (P-Value 0.034) and electrolysis time (0.052) is crucial for the (Al-Al) electrode, as shown in Table 4. ANOVA results for the (Al-Fe) electrode showed important factors with time = 0.011 and pH = 0.014. For the (Fe-Fe) electrode, key factors were C.D. and pH at 0.001, D.E. = 0.014, and I.C. = 0.041 for turbidity removal efficiencies, ranked as initial pH > current density > electrolysis time..Confirmation analysis of variance (ANOVA)

experiments were conducted a single time to carefully verify the outcomes while ensuring all conditions remained consistent throughout the process [53].

3.7.1. Regression Model

ANOVA and linear regression thoroughly identified significant model terms, demonstrating notable statistical significance in the mode characterized by P-value, R2, adjusted R^2, and predicted R^2 for various electrode types as detailed in Table (9). This analysis highlights the relevant factors influencing the outcomes, underscoring the importance of these statistical measures in understanding the relationships between the variables studied [54].

Table 9: Linear regression model values according to types of electrodes

Model summary	(Fe-Fe) electrodes	(Al-Al) electrodes	(Al-Fe) electrodes
S	1.943	3.968	3.335
R-sq	9.92	9.57	9.71
R-sq(adj)	9.92	9.55	9.70

$$Predict\ \%R\ (Fe-Fe) = 63.503 - 11.94X1 - 21.49X2 - 6.01\,X\,3 - 1.05X4 - 18.25X5 \quad (7)$$

$$Predict\ \%R\ (Al-Al) = 81.33 - 17.79\,X1 - 19.79\,X2 - 16.49\,X3 \quad (8)$$

$$Predict\ \%R\ (Al-Fe) = 67.81 - 12.29\,X2 - 26.53X3 \quad (9)$$

The ANOVA results in Table 10 show that at the 5% significance level, terms X1, X2, X3, and X4 are significant for predicting %R (Fe-Fe), while X1, X2, and X3 are significant for %R (Al-Al). X4 and X5 are not significant for predicting %R (Al-Fe).

Table 10: ANOVA results Analysis. Linear Regression Model: [%R versus I.C., pH, Time, C., D for (Al-Al) electrode].

Source	DF	Adj SS	Adj MS	F-Value	P-Value
I.C.	4	1708.3	427.08	5.68	0.060
pH	4	2407.2	601.79	8.01	0.034
Time	4	1874.7	468.68	6.24	0.052
C.D	4	1015.8	253.96	3.38	0.133
D. E.	4	522.2	130.54	1.74	0.303
=Error	4	300.5	75.13		
Total	24	7828.7			

Table 11: ANOVA results Analysis. Linear Regression Model: [%R versus I.C., pH, Time, C., D for (Al-Fe) electrode].

Source	DF	Adj SS	Adj MS	F-Value	P-Value
I.C.	4	642.7	160.69	2.44	0.204
pH	4	3512.2	878.05	13.33	0.014
Time	4	4039.3	1009.82	15.33	0.011
C.D.	4	473.9	118.47	1.80	0.292
D. E.	4	329.0	82.24	1.25	0.417
Error	4	263.4	65.86		
Total	24	9260.5			

Table 12: ANOVA results Analysis. Linear Regression Model: [%R versus I.C., pH., Time, C., D for (Fe-Fe) electrode].

Source	DF	Adj SS	Adj MS	F-Value	P-Value
I.C.	4	643.6	160.91	7.17	0.041
pH	4	4836.4	1209.09	53.84	0.001
C.D.	4	4833.6	1208.41	53.81	0.001
D.E.	4	1172.1	293.02	13.05	0.014
TIME	4	500.0	125.01	5.57	0.063
Error	4	89.8	22.46		
Total	24	12075.6			

Tables (9-12) provide a comprehensive overview of the Response Tables that present the Signal-to-Noise (S/N) Ratios along with the Mean Removal Percentage (%R) for each factor and level being analyzed. The primary objective is to achieve Maximum Dye Removal, which is guided by the criterion known as "Larger is Better" for the S/N ratio. Through a careful examination of several observations found in these Tables, various insights can be derived and analyzed regarding the factors and their respective levels.

A. Factor Significance (Delta and Rank)

The most critical information is the Delta (Δ) value and the Rank. The Δ value represents the difference between the highest and lowest average S/N ratio for a factor. A larger Δ value indicates a greater influence on EC process stability and performance. The analysis consistently identifies pH (Rank 1) and Current Density (C.D.) (Rank 2) as the key factors across all electrode materials (Fe-Fe, Al-Al, or Fe-Al). The chemistry of coagulant species (pH-dependent) and the rate of coagulant generation (C.D.-dependent Fen+ or Al3+ production) dominate EC for Malachite Green removal.

B. Optimizing Factor Levels (Max S/N Ratio)

The optimal level for each factor is the one that yields the highest average S/N ratio (and also the highest mean %*R*) as shown in Table 13 below

Table 13: Optimum level results obtained according to electrode mode

Electrode System	Optimal Level for pH	Optimal Level for Current Density mA/cm2	Optimal Level for Time(min)
Fe-Fe	10	1.0	20
Al-Al	8	0.8	60
Al-Fe (mixed)	10	0.8	60

Iron electrodes require shorter times (20 min) and higher C.D. (1.0 mA/cm^2) due to the quick formation of dense flocs ($Fe(OH)_3$) that rapidly remove contaminants. An optimal pH of 10 enhances the effective adsorption of $Fe(OH)_3$ precipitates.

Aluminum electrodes need longer times (60 min) and lower C.D. (0.8mA/cm^2). Aluminum hydroxides ($Al(OH)_3$) form larger, voluminous flocs more slowly but effectively trap smaller particles like dye molecules. The optimal pH of 8 is near the isoelectric point of $Al(OH)_3$, minimizing surface charge and enhancing aggregation.

Fe-Al (Mixed): This system blends requirements, needing longer time and lower C.D. like Al-Al, while optimal pH is high (pH 10) like Fe-Fe. The Fe anode influences coagulant chemistry at high pH, but performance is affected by the different dissolution rate and charge demand of the Al cathode, or vice versa, based on EC setup.

3.8 Comparison between Electrode Types

Fe–Fe electrodes showed the highest removal efficiency (>99%), followed by Al–Al (>97%) and Al–Fe (>90%). Iron electrodes produced denser flocs with better settling, while aluminum generated smaller but highly charged flocs for effective MG removal. Mixed Al–Fe electrodes had moderate performance due to varying dissolution rates. ANOVA confirmed that pH and electrolysis time were significant in all electrode systems ($p < 0.05$).

3.9 Predicted vs Experimental Results

Predicted removal efficiencies from Taguchi regression models were compared to experimental values, showing a deviation within an acceptable range (<5%), which indicates strong model accuracy. The high correlation confirms Taguchi design's effectiveness in optimizing electrocoagulation performance. Table 14 shows comparisons between predicted and experimental % removal, highlighting the best deviation based on electrode type.

Table 14: The comparisons between predicted & Experimental % removal with best deviation depending upon type of electrodes

Electrode	Predicted %R	Experimental %R	Best Deviation
Fe–Fe	100%	98.6%	<1.5%
Al–Al	100%	96.8–100%	<3%
Al–Fe	88–92%	88–92.5%	<2%

Residual probability diagrams (Figure 6 a, b) are essential for detecting systematic deviations, assuming errors are independent and normally distributed. They show homogeneity of error variance 28; fewer errors mean points are closer to the line, as illustrated in Figure 6 a, b.

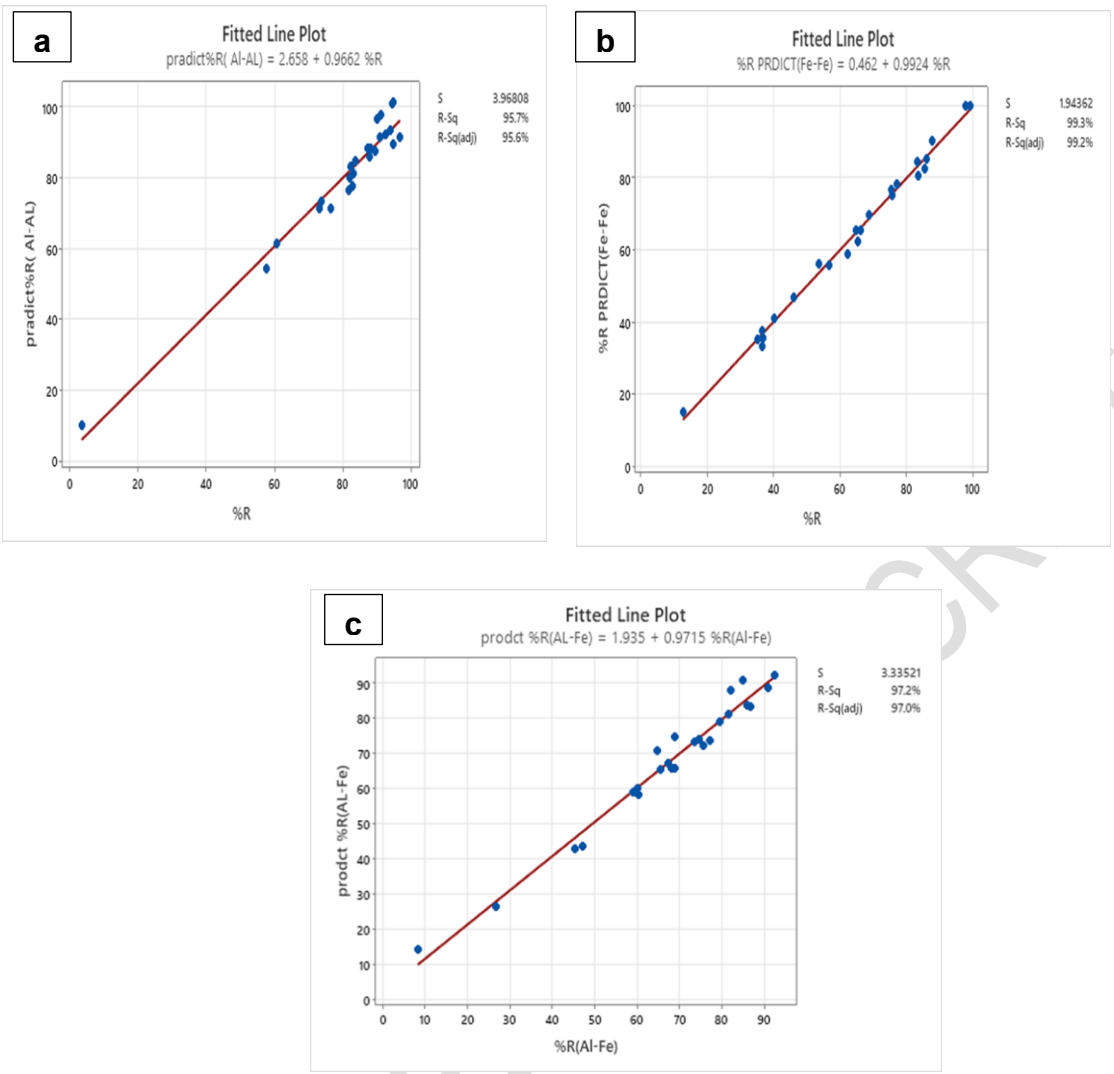

Figure 6: Predicted versus actual value plotted (a) (Al-Al) electrode (b), (Fe-Fe) electrode, and (c) (Al-Fe) electrode.

Figure 6 shows the data from Tables 9 and 10, confirming the optimal levels and their significance.

The steeper line slope indicates a greater factor influence on performance (S/N ratio). pH and C.D. have the steepest slopes, confirming their top ranks, while Initial Concentration and Electrode Distance show lower influence[55]. Each plot's peak confirms optimal levels for each electrode type. The Fe-Fe system shows a sharp increase in Time up to 20 min, while the Al-Al system peaks around pH 8.

Comparing the plots shows that shifting the pH significantly affects the S/N ratio more than changing the electrode distance. Figure 6 visually confirms the conclusions from Tables 9 and 10, aiding in selecting optimal process parameters.

4. Conclusion

Electrocoagulation removed Malachite Green dye from water using Fe–Fe, Al–Al, and Al–Fe electrodes. Taguchi design optimized the process, while ANOVA found pH and electrolysis time as key factors ($p < 0.05$). Fe–Fe achieved the highest removal rate (>99%)..Predicted and actual values closely matched, confirming Taguchi modeling's reliability. The study validates electrocoagulation with statistical optimization as an effective solution for dye-laden wastewater treatment.

Future studies should: (1) evaluate real wastewater with mixed dyes and contaminants, (2) test more electrode materials and hybrid setups, (3) use advanced machine learning for optimization, and (4) analyze sludge characteristics and environmental impacts for large-scale application (5) The use of continuous systems (6) .The use of combined treatment processes**.**

References

[1]Ozyonar, F., Muratcobanoglu, H., & Gokkus, O. (2017). Taguchi approach for color removal using electrocoagulation with different electrode connection types. Fresenius Environ Bull, 26(12), 7600-7.

[2] Abbas, S.H., Ridha, A.M., Rashid, K.H., Khadom, A.A., (2023),Biosorption of Congo red dye removal from aqueous solution using fennel seed spent and garlic peel, *International Journal of Environmental Science and Technology*, 20(12), pp. 13845–13858

[3] Márquez, A. A., Coreño, O., & Nava, J. L. (2022). A hybrid process combining electrocoagulation and active chlorine-based photoelectro-Fenton-like methods during the removal of Acid Blue 29 dye. *Journal of Electroanalytical Chemistry*, *922*, 116732, https://doi.org/10.1016/j.jelechem.2022.116732

[4] Ibrahim,M.S., Abbas,S.H., Al-Shami,A.,(2023),Taguchi approach for electrocoagulation for treatment of methyl red dye from textile wastewater by using different connection electrodes, *Desalination and Water Treatment*, 297, pp. 240–253

[5] Younis, Y.M., Abbas, S.H., Najim, F.T., Kamar, F.H., Nechifor, G , (2020), Comparison of an artificial neural network and a multiple linear regression in predicting the heat of combustion of diesel fuel based on hydrocarbon groups , Revista De ChimieOpen source preview, 71(6), pp. 66–74

[6] Shakor, Z. M., Mahdi, H. H., Al-Sheikh, F., Alwan, G. M., & Al-Jadir, T. (2021). Ni, Cu, and Zn metal ions removal from synthetic wastewater using a watermelon rind (Catullus landaus). Materials Today: Proceedings, 42, 2502-2509. https://doi.org/10.1016/j.matpr.2020.12.570

[7] Alemu, T., Mekonnen, A., & Leta, S. (2019). Integrated tannery wastewater treatment for effluent reuse for irrigation: Encouraging water efficiency and sustainable development in developing countries. *Journal of Water Process Engineering*, *30*, 100514, https://doi.org/10.1016/j.jwpe.2017.10.014

[8] Deng, D., Lamssali, M., Aryal, N., Ofori-Boadu, A., Jha, M. K., & Samuel, R. E. (2020). Textiles wastewater treatment technology: A review. Water Environment Research, 92(10), 1805-1810. https://doi.org/10.1002/wer.1437

[9] Manikandan, S., & Saraswathi, R. (2023). Textile dye effluent treatment using advanced sono-electrocoagulation techniques: A Taguchi and particle swarm optimization modeling approach. ENERGY SOURCES, PART A: RECOVERY, UTILIZATION, AND

ENVIRONMENTAL EFFECTS, 2(45), 4501-4519. https://doi.org/10.1080/15567036.2023.2205356
[10] Verma, A. K., Dash, R. R., & Bhunia, P. (2012). A review on chemical coagulation/flocculation technologies for removal of colour from textile wastewaters, Journal of environmental management, 93(1), 154-168, https://doi.org/10.1016/j.jenvman.2011.09.012
[11] Ibrahim, M.S., Abbas, S.H., Beddai, A.A.,(2022), Response Surface mythology for Electrocoagulation Treatment for Methyl Red Dye from Wastewater through an Fe and Al Polar, *AIP Conference Proceedings*, 2660, 020086
[12] Linares-Hernández, I., Barrera-Díaz, C., Bilyeu, B., Juárez-GarcíaRojas, P., & Campos-Medina, E.,(2010), A combined electrocoagulation–electrooxidation treatment for industrial wastewater, Journal of hazardous materials, 175(1-3), 688-694. https://doi.org/10.1016/j.jhazmat.2009.10.064
[13] AL-Mashhadi, R. N., & Al-Obaidy, A. (2022, November). Malachite green removal from wastewater by electro coagulation treatment technique, In AIP Conference Proceedings, Vol. 2660, No. 1, AIP Publishing, https://doi.org/10.1063/5.0109531
[14] Abbas, S.H., Younis, Y.M., Rashid, K.H., Khadom, A.A., (2022),Removal of methyl orange dye from simulated wastewater by electrocoagulation technique using Taguchi method: kinetics and optimization approaches, *Reaction Kinetics, Mechanisms and Catalysis*
[15] Ghernaout, D., Naceur, M. W., & Ghernaout, B. (2011). A review of electrocoagulation as a promising coagulation process for improved organic and inorganic matters removal by electrophoresis and electroflotation, Desalination and Water Treatment, 28(1-3), 287-320. https://doi.org/10.5004/dwt.2011.1493
[16]Abbas, S.H., Younis, Y.M., Hussain, M.K., ...Nechifor, G., Pasca, B.,(2020), Utilization of waste of enzymes biomass as biosorbent for the removal of dyes from aqueous solution in batch and fluidized bed column, *Revista de Chimie*,71(1), pp. 1–12
[17] Nandoost, A., Bahramifar, N., Moghadamnia, A. A., & Kazemi, S. (2022). Adsorption of Malachite Green (MG) as a Cationic Dye on Amberlyst 15, an Ion-Exchange Resin. Journal of Environmental and Public Health, 2022(1), 4593835, https://doi.org/10.1155/2022/4593835.
[18] Kamar, F.H., Abbas, S.H., Mohammed, A.H., Craciun, M.E., Nechifor, A.C.,(2018), Isotherm and kinetic models for bio-sorption of cadmium ions from aqueous solutions using dry peanut shells and hazelnut shells, *Revista de Chimie*, 69(10), pp. 2603–2607
[19] Naje, A. S., Chelliapan, S., Zakaria, Z., Ajeel, M. A., & Alaba, P. A. (2017). A review of electrocoagulation technology for the treatment of textile wastewater Reviews in Chemical Engineering, 33(3), 263-292. https://doi.org/10.1515/revce-2016-0019
[20] Abbas, S.H., Ali, W.H.,(2018), Evaluation of biomass type blue cyanophyta algae for the sorption of Cr(III), Zn(II) and Ni(II) from aqueous solution using batch operation system: Equilibrium, kinetic and thermodynamic studies, *Global Nest Journal*, 20(1), pp. 69–82
[21] Getaye, M., Hagos, S., Alemu, Y., Tamene, Z., & Yadav, O. P. (2017). Removal of malachite green from contaminated water using electro-coagulation technique, Journal of analytical & pharmaceutical research, 6(4), 00184, https://doi.org/10.15406/japlr.2017.06.00184
[22] Akhtar, A., Aslam, Z., Asghar, A., Bello, M. M., & Raman, A. A. A. (2020). Electrocoagulation of Congo Red dye-containing wastewater: Optimization of operational parameters and process mechanism. Journal of Environmental Chemical Engineering, 8(5), 104055. https://doi.org/10.1016/j.jece.2020.104055.
[23] Ahmad, T., Manzar, M. S., Khan, S. U., Kazi, I. W., Mu'azu, N. D., & Ullah, N. (2023). Synthesis and adsorptive performance of a novel triazine core-containing resin for the

ultrahigh removal of malachite green from water. Arabian Journal for Science and Engineering, 48(7), 8571-8584. https://doi.org/10.1007/s13369-022-07015-w.
[24] Amaku, J. F., & Taziwa, R. (2024). Sequestration of chromium by Ananas comosus extract–coated nanotubes: synthesis, characterization, optimization, thermodynamics, kinetics, and antioxidant activities. Biomass Conversion and Biorefinery, 1-16. https://doi.org/10.1007/s13399-023-05210-9.
[25] Asghar, A., Abdul Raman, A. A., & Daud, W. M. A. W. (2014). A comparison of central composite design and Taguchi method for optimizing Fenton process. The Scientific World Journal, 2014(1), 869120. https://doi.org/10.1155/2014/869120.
[26] Praveena, S. M., Rashid, U., & Abdul Rashid, S. (2022). Optimization of nutrients removal from synthetic greywater by low-cost activated carbon: application of Taguchi method and response surface methodology. Toxin Reviews, 41(2), 506-515. https://doi.org/10.1080/15569543.2021.1903037.
[27] Karimifard, S., & Moghaddam, M. R. A. (2018). Application of response surface methodology in physicochemical removal of dyes from wastewater: a critical review. Science of the Total Environment, 640, 772-797. https://doi.org/10.1016/j.scitotenv.2018.05.355.
[28] Shojaei, S., Shojaei, S., Band, S. S., Farizhandi, A. A. K., Ghoroqi, M., & Mosavi, A. (2021). Application of Taguchi method and response surface methodology into the removal of malachite green and auramine-O by NaX nanozeolites. Scientific reports, 11(1), 16054. https://doi.org/10.1038/s41598-021-95649-5.
[29]. Rajabizadeh A., Abdipour H. , Hossein Mansoorian J.,(2025), A new approach for the elimination of Rhodamine B dye using a combination of activated persulfate and dithionite in the presence of magnetic fields, Chemical Engineering and Processing - Process Intensification, Volume 209, 110160, https://doi.org/10.1016/j.cep.2025.110160
[30] Asgari G, SeidMohammadi A, Rahmani A, Shokoohi R , Abdipour.H. ,(2024), Concurrent elimination of arsenic and nitrate from aqueous environments through a novel nanocomposite: Fe_3O_4-ZIF8@eggshell membrane matrix, Journal of Molecular Liquids, Volume 411, 125810, https://doi.org/10.1016/j.molliq.
[31] Arslan, H., Salici, K., Gün, M., & Yalvaç, M. (2021). Investigation of the usability of the electrocoagulation method in malachite green removal from water solution. Environmental Research and Technology, 6(3), 218-225. https://doi.org/10.35208/ert.1210044
[32] Shojaei, S., Shojaei, S., Band, S. S., Farizhandi, A. A. K., Ghoroqi, M., & Mosavi, A. (2021). Application of Taguchi method and response surface methodology into the removal of malachite green and auramine-O by NaX nanozeolites. Scientific reports, 11(1), 16054. https://doi.org/10.1038/s41598-021-95649-5
[33] Vrsalović, L., Medvidović, N. V., Svilović, S., & Pavlinović, A. (2023). Taguchi method in the optimization of municipal wastewater treatment by electrocoagulation integrated with zeolite. Energy reports, 9, 59-76. https://doi.org/10.1016/j.egyr.2023.03.086.
[34] Yang, Z. H., Xu, H. Y., Zeng, G. M., Luo, Y. L., Yang, X., Huang, J., ... & Song, P. P. (2015). The behavior of dissolution/passivation and the transformation of passive films during electrocoagulation: Influences of initial pH, Cr (VI) concentration, and alternating pulsed current. Electrochimica Acta, 153, 149-158. https://doi.org/10.1016/j.electacta.2014.11.183.

[35] Fadhil, H.; Abbas, S., Al-Sheikh, F. ;(2025); Electrocoagulation-Assisted Fenton Reagent as Advanced Oxidation Processes used for Degradation of Organic Pollutants from Industrial Wastewater: A Review; Chemistry Africa , DOI: 10.1007/s42250-025-01213-3

[36] Liao D. , Tian G., Xiaoyu F., Li Z., Su Y. , Chang W. , Chang W.,(2025), Toward an Active Site–Performance Relationship for Oxide-Supported Single and Few Atoms, ACS Catalysis , 15, 10, 8219–8229, doi: 10.1021/acscatal.5c00981

[37] LiY. , Bu J. , SunY. , Huang Z. , Zhu X. , Li S. , Chen P. , Tang Y. , He G. , Zhong S.,(2025), Efficient degradation of norfloxacin by synergistic activation of PMS with a three-dimensional electrocatalytic system based on Cu-MOF, Separation and Purification Technology, Volume 356, Part B, 1, 129945, doi: https://doi.org/10.1016/j.seppur.2024.129945

[38] Guo X. , Guan Q. , Jiang W. , Zhang H. , Du D., (2025), Experimental design of $La(OH)_3$-zeolite modified wood ceramics for adsorption of total phosphorus in water and its composite properties study, Desalination and Water Treatment, Volume 324, , 101489, doi: https://doi.org/10.1016/j.ijoes.2023.01.005

[39] Geng H. , Chen T. , Chen J. , Huang B., Wang G.,(2025), Temperature effects on single cavitation bubble dynamics under the free field condition: Experimental and theoretical investigations on water, Ultrasonics Sonochemistry, Volume 120, 107520, https://doi.org/10.1016/j.ultsonch.2025.107520

[40] Xiong J., Hu Q., Wu J. ,Jia Z., Ge S., Cao Y., Zhou J., Wang Y., Yan J. , Xie L., ChaiX., Zhang L. , (2023), Structurally stable electrospun nanofibrous cellulose acetate/chitosan biocomposite membranes for the removal of chromium ions from the polluted water, Advanced Composites and Hybrid Materials, 6(3), DOI:10.1007/s42114-023-00680-x

[41] Du G., Wang S., Xu K., (2023), Structurally stable electrospun nanofibrous cellulose acetate/chitosan biocomposite membranes for the removal of chromium ions from the polluted water, Advanced Composite and Hybrid Materials, 6: 99.

[42] Bing B., Fan B., Xianke L., Qingke N., Xiangxin J..,(2022), The remediation efficiency of heavy metal pollutants in water byindustrial red mud particle waste. Environmental Technology & Innovation, 28: 102944

[43] Maruthai, S.; Rajendran, S.; Selvanarayanan, R.; Gowri, S., (2025),Wastewater Recycling Integration with IoT Sensor Vision for Real-time Monitoring and Transforming Polluted Ponds into Clean Ponds using HG-RNN", Global NEST Journal. 27(4), https://doi.org/10.30955/gnj.06758

[44] Selvanarayanan R., Rajendran S., Pappa C. K. and Thomas B.,(2025),Wastewater Recycling to Enhance Environmental Quality using Fuzzy Embedded with RNNIoT for Sustainable Coffee Farming". Global NEST Journal, Vol 26, No 8, 06346 https://doi.org/10.30955/gnj.06346.

[45] Sivasubramanian S. , Venkatesan S. , Thanarajan T. , Rajendran S. ,(2025), Al-Biruni Earth Radius Optimization for enhanced environmental data analysis in remote sensing imagery. Agrociencia,, pp.1-18. . DOI: https://doi.org/10.47163/agrociencia.v59i5.3380,

[46] Bani-Melhem K. · Alnaief M. · Al-Qodah Z. · Al-Shannag M. · Elnakar H. · AlJbour N. · Alu'datt M. · Alrosan M., · Ezelden E., (2025), On the performance of electrocoagulation treatment of high-loaded gray water: kinetic modeling and parameters optimization via response surface methodology, Applied Water Science , 15:114, https://doi.org/10.1007/s13201-025-02451-z

[47] Bani-Melhem K. , Al-Shannag M , Alrousan D., Al-Kofahi S. , Zakaria Al-Qodah Z. , Al-Kilani M, (2017), Impact of soluble COD on grey water treatment by electrocoagulation technique, Desalination and Water Treatment, Volume 89, 9, Pages 101-110, https://doi.org/10.5004/dwt.2017.21379

[48] Al-Qodah Z. , Al-Shannag M. , Hudaib B. , Bani Salameh W., . Shawaqfeh A., Assirey E. , (2025), Synergy and enhanced performance of combined continuous treatment processes of pre-chemical coagulation (CC), solar-powered electrocoagulation (SAEC), and post-adsorption for Dairy wastewater, Case Studies in Chemical and Environmental Engineering, Volume 11, 6, 101183, https://doi.org/10.1016/j.cscee.2025.101183

[49] Al-Qodah Z. , AL-Rajabi M., Al Amayreh H., Assirey E., Bani-Melhem K., Al-Shannag M., (2025), Performance of Continuous Electrocoagulation Processes (CEPs) as an Efficient Approach for the Treatment of Industrial Organic Pollutants: A Comprehensive Review, *Water* , *17*(15), 2351; https://doi.org/10.3390/w17152351

[50] Hussain, M.K., Abbas, S.H., Younis, Y.M., Rahman, M.A., Jamil, T., (2021), Fabrication of epoxy composite material reinforced with bamboo fibers, Journal of Applied Engineering 19(1), pp. 119–124

[51] Liu, N., Dai, W., Fei, F., Xu, H., Lei, J., Quan, G, Zheng, Y; Zhang, X.,Tang, L. (2022). Insights into the photocatalytic activation persulfate by visible light over ReS2/MIL-88B (Fe) for highly efficient degradation of ibuprofen: Combination of experimental and theoretical study, Separation and Purification Technology, 297, (9), p. 121545

[52] Ammar, M., Yousef, E., Ashraf, S., Baltrusaitis, J. (2024), Removal of inorganic pollutants and recovery of nutrients from wastewater using electrocoagulation: a review. Separations, 11(11), DOI:10.3390/separations11110320

[53] Arunachalam, S. J., Saravanan, R., Sathish, T., Alarfaj, A. A., Giri, J., Kumar, A. (2024) , Enhancing mechanical performance of MWCNT filler with jute/kenaf/glass composite: a statistical optimization study using RSM and ANN. Materials Technology, 39(1),p. 2381156

[54] Agrawal, J. P., Somani, N., & Gupta, N. K., (2026), Optimizing electric discharge machining parameters using Taguchi method and ANOVA: A study on AISI D2 steel machining with copper electrodes and materials science progress, Next Materials. Volume 10, (1),p. 101361, https://doi.org/10.1016/j.nxmate

[55]Liu, Q., Liu, S., Wang, D., Sun, D., Ge, Y., Zhang, S, Li G., Jho E., Joo J. , Zhao X., Ye M., Hu J.,(2025). Decoupling soil pH and geography: Universal drivers of cadmium bioavailability in rice across terrains, Journal of Environmental Management, 381(5), p. 125297, DOI: 10.1016/j.jenvman.2025.125297